Optimal Homogeneous Transmission Line Model for Graphene Interconnects

A. Maffucci, A. Tamburrino, S. Ventre
Department of Electrical and Information Engineering
University of Cassino and Southern Lazio, Cassino, Italy
maffucci@unicas.it

***Abstract*— The paper presents a novel technique to derive an equivalent homogeneous transmission line model of a lossy electrical interconnect embedding a graphene contact. The technique is based on the exploitation of the monotonicity property that holds for suitable matrices associated to the transmission line model. Starting from simulated or measured values of any of the terminal matrices describing the original line (*e.g.*, impedance, admittance or scattering matrices), equivalent permittivity values are obtained by checking the behavior of an index related to such matrices. These values correspond to homogeneous transmission lines whose features (such as stored energy, propagation velocity, and characteristic impedance) provide lower and upper bound to the optimal performance. The technique is here applied to an interconnect embedding a graphene contact, which introduces a huge variability of the permittivity value.**

Keywords*— Graphene interconencts; Inhomogeneous media; Homogenization techniques; Interconnects; Transmission Lines.

I. Introduction

Modeling the signal propagation along a multiconductor interconnect embedded in inhomogeneous media is a classical problem that has been approached with different techniques [1]. Fully-numerical models based on differential formulations (e.g., FDTD) can naturally handle inhomogeneous media but usually require a large domain to be meshed, including conductors and dielectrics. On the other side, methods based on integral formulations (e.g., EFIE) require meshing only the conducting regions, but suffer from the cumbersome computational cost associated to the Green functions for inhomogeneous media, usually derived from costly evaluation of Sommerfeld integrals [2]-[3].

In presence of inhomogeneous media, also the popular Transmission Line (TL) model must be modified to take into account the physical features of the guided propagating field, which is not of Transverse ElectroMagnetic (TEM) type, as in the case of an interconnect embedded in homogeneous media [4]-[5]. However, under the quasi-TEM assumption is it still possible to model the inhomogeneous interconnect in the frame of the TL theory. By using such a model, the propagation along a Multiconductor Transmission Line (MTL) made by N signal conductors and one ground conductor is associated to N different modes, each of them characterized by a different velocity [4]-[5]. This is the main difference with respect to the homogeneous case, where all the modes propagate with the same velocity:

$$v = 1/\sqrt{\varepsilon\mu} \quad (1)$$

being ε and μ the permittivity and permeability of the surrounding medium. The presence of different propagation velocities introduces a rather high complexity in any circuit model derived from the TL model of the interconnect, due to high number of pole and residues needed to catch accurately the phase variation associated with the propagation delays. Therefore, popular macromodeling techniques such as the Vector Fitting [6], have been modified to take into account explicitly the propagation delays, *e.g.* [7]. In many cases, however, it could be useful to describe such interconnects through simpler models that can be easier and faster simulated: this may happen, for instance, when extensive signal integrity analysis of large interconnects systems must be performed, and time-consuming task must be implemented, such as the analysis of the eye-diagrams [8]. Another case is given by the statistical analysis of the signal integrity of such systems, for instance to take into account the variability induced by the manufacturing process [9].

Practical examples of inhomogeneous interconnects are given, for instance, by electrical cables with many dielectric coatings, or by electrical traces embedded in two or more dielectric layers (*e.g.*, PCB or on-chip interconnects). In this paper, we focus on hybrid interconnects made by conventional materials and novel nanomaterials, such as graphene, which are nowadays widely studied, in view of their potentially outstanding performance [10]-[11]. Indeed, the presence of such materials introduce a strong variability of the physical parameters, such as conductivity or permittivity.

In this paper, we derive a simplified macromodel by using homogenization techniques. The concept of equivalent homogeneous system is widely used in electromagnetics to lower the computational cost of simulations, for instance when dealing with highly non-uniform materials such as the composites or the metamaterials. An example is the homogenization of non-uniform TLs proposed in [12], based on Principal Component Analysis.

The technique adopted here has been proposed by the Authors in [13] to homogenize MTLs embedded in inhomogeneous dielectrics. It is based on the property of monotonicity of some matrix operators associated to this model, with respect to the permittivity value. The main features are summarized in Section II. We use here such a technique to derive the equivalent permittivity values associated to a microstrip embedding graphene nanoplatelets, described in Section III. The results, shown in Section IV, highlight a very good agreement with respect to those obtained in literature.

II. MACROMODELING VIA MONOTONICITY

In the following, we briefly recall the results shown in [13], where an equivalent permittivity value is derived, by using the monotonicity property of some matrices associated to the MTL model of an inhomogeneous interconnect. Specifically, the inhomogeneity comes from the presence of a spatial non-uniform electrical permittivity, $\varepsilon = \varepsilon(\boldsymbol{r})$.

A. The Monotonicity property

The homogenization procedure may start from any multiport representation of a lossy MTL with *N* signal lines and a ground one (Fig.1): let us consider, for instance the terminal impedance matrix, **Z,** or the admittance one, **Y**, defined as:

$$\begin{bmatrix}\mathbf{V}_0\\ \mathbf{V}_l\end{bmatrix}=\begin{bmatrix}\mathbf{Z}_s & \mathbf{Z}_m\\ \mathbf{Z}_m & \mathbf{Z}_s\end{bmatrix}\begin{bmatrix}\mathbf{I}_0\\ \mathbf{I}_l\end{bmatrix},\quad \begin{bmatrix}\mathbf{I}_0\\ \mathbf{I}_l\end{bmatrix}=\begin{bmatrix}\mathbf{Y}_s & \mathbf{Y}_m\\ \mathbf{Y}_m & \mathbf{Y}_s\end{bmatrix}\begin{bmatrix}\mathbf{V}_0\\ \mathbf{V}_l\end{bmatrix}, \qquad (2)$$

where $\mathbf{V}_a(\mathbf{I}_a)$ is the vector of the *N* voltages (currents), evaluated at the two line ends (subscripts "0" and "*l*"), being *l* the line length, Fig.1. The MTL theory provides [4]-[5]:

$$\mathbf{Z}_S\mathbf{Z}_M^{-1} = -\mathbf{Y}_M^{-1}\mathbf{Y}_S = \cosh(\mathbf{K}l), \qquad (3)$$

$$-\mathbf{Y}_M^{-1}\mathbf{Z}_M = \sinh(\mathbf{K}l)\mathbf{Z}_0\sinh^{-1}(\mathbf{K}l)\mathbf{Z}_0, \qquad (4)$$

where the propagation operator $\boldsymbol{K}$ and the characteristic impedance matrix $\mathbf{Z_0}$ are, in turns, related to the per-unit-length parameter matrices [4]-[5]:

$$\mathbf{K} = -i\omega[\mathbf{Z}'\mathbf{Y}']^{1/2},\ \mathbf{Z}_0 = [(\mathbf{Y}')^{-1}\mathbf{Z}']^{1/2}. \qquad (5)$$

By exploiting the physical properties of these latter operators, it is possible to prove that the following matrices:

$$\mathbf{X_1} = Im\{acosh[\lambda(\mathbf{Y}_m^{-1}\mathbf{Y}_s)]\}, \qquad (6)$$

$$\mathbf{X_2} = Re\{-\mathbf{Y}_m^{-1}\mathbf{Z}_m\}, \qquad (7)$$

are monotonic in a "weak sense", with respect to the permittivity [13]. This means that the following property holds:

$$\varepsilon_1(\boldsymbol{r}) \geq \varepsilon_2(\boldsymbol{r})\ \forall\boldsymbol{r} \rightarrow \lambda_k(\mathbf{X_1}) \geq \lambda_k(\mathbf{X_2})\ \forall k \qquad (8)$$

where λ_k are the eigenvalues of the matrices.

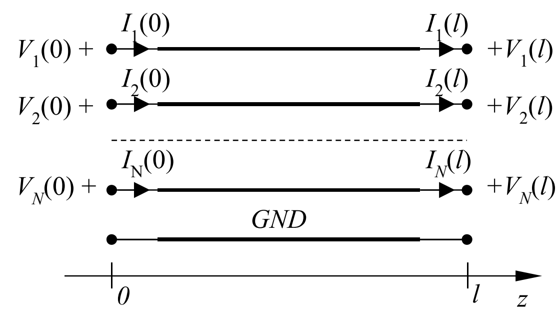

Fig. 1. Multiconductor transmission line, with voltages and currents references.

B. Macromodeling and optimization

The proposed technique aims at macromodeling the inhomogeneous TL in terms of equivalent single homogeneous ones, thus described by a single value of the propagation velocity (or propagation delay). The concept of optimization is associated to target quantities, whose values obtained in the equivalent line must be compared to that in the original line, as done in classical works like [14].

Here the optimization is contemporarily carried out from the physical standpoints of the stored energy, U, the propagation velocity, v, and the characteristic impedance, $\mathbf{Z}_0$. Specifically, we are seeking two uniform values of the permittivity, $\bar{\varepsilon}_1$ and $\bar{\varepsilon}_2$, such that the solutions of the two homogeneous lines associated to them can bound those of the original line:

$$U_1 \leq U \leq U_2,\ \ v_1 \leq v_k \leq v_2,\ \ \mathbf{Z}_{01} \leq \mathbf{Z}_0 \leq \mathbf{Z}_{02}. \qquad (9)$$

In other words, $\bar{\varepsilon}_1$ and $\bar{\varepsilon}_2$ are the bounds for the optimal value of the equivalent permittivity, in terms of the quantities (9).

Note that for two matrices **A** and **B**, the relation $\mathbf{A} \leq \mathbf{B}$ means that the eigenvalues of $\mathbf{A} - \mathbf{B}$ are all non-positive.

To identify the above two values of permittivity, it is necessary to study the variation of the sign of the following index associated to the matrices $\mathbf{X_1}$ and $\mathbf{X_2}$ defined in (6)-(7):

$$s_W(\bar{\varepsilon}) = \frac{\sum_{i=1}^{M}\lambda_i(\tilde{\mathbf{X}}) - \lambda_i(\mathbf{X}_{\bar{\varepsilon}})}{\sum_{i=1}^{M}\left|\lambda_i(\tilde{\mathbf{X}}) - \lambda_i(\mathbf{X}_{\bar{\varepsilon}})\right|}. \qquad (10)$$

Here $\tilde{\mathbf{X}}$ denotes any of the matrices $\mathbf{X_1}$ or $\mathbf{X_2}$ referred to the original inhomogeneous line with permittivity, $\varepsilon(\boldsymbol{r})$, whereas $\mathbf{X}_{\bar{\varepsilon}}$ is the corresponding matrix associated to a line with a uniform value of permittivity, $\varepsilon(\boldsymbol{r}) = \bar{\varepsilon}$.

Given its expression (10), it is easy to realize that the index is bounded: $|s_W| \leq 1$. In addition, it can be proven [13] that the sign index s_W is equal to +1 for $\bar{\varepsilon} \leq \bar{\varepsilon}_1$, to -1 for $\bar{\varepsilon} \geq \bar{\varepsilon}_2$, and it is $|s_W| < 1$ when $\bar{\varepsilon}_1 < \bar{\varepsilon} < \bar{\varepsilon}_2$. As a consequence, the requested values of the permittivity $\bar{\varepsilon}_1$ and $\bar{\varepsilon}_2$ can be identified as the extremals of the *transition region* $|s_W| < 1$.

In order to bound the original line in agreement with the inequalities in (9), the above study must be performed both for the matrices $\mathbf{X_1}$ and $\mathbf{X_2}$ in (6)-(7). This study provides two intervals: $(\bar{\varepsilon}_{11}, \bar{\varepsilon}_{21})$ for $\mathbf{X_1}$, $(\bar{\varepsilon}_{12}, \bar{\varepsilon}_{22})$ for $\mathbf{X_2}$. The final values will be given by the extremals of the set obtained by the union of the two intervals:

$$\bar{\varepsilon}_1 = min\ \{(\bar{\varepsilon}_{11}, \bar{\varepsilon}_{21}) \cup (\bar{\varepsilon}_{12}, \bar{\varepsilon}_{22})\}, \qquad (11)$$

$$\bar{\varepsilon}_2 = max\ \{(\bar{\varepsilon}_{11}, \bar{\varepsilon}_{21}) \cup (\bar{\varepsilon}_{12}, \bar{\varepsilon}_{22})\}. \qquad (12)$$

Note that the proposed technique only requires the knowledge at a single frequency point of any of the terminal matrices **Z** or **Y** of the original inhomogeneous system, either provided by simulations or measurements. As for the equivalent homogeneous models corresponding to a uniform permittivity, $\bar{\varepsilon}$, the required matrices can be easily obtained by applying the MTL model.

III. Analysis of a Graphene Interconnect

A. A microstrip embedding a graphene contact

The graphene interconnect analyzed here has been described in [15] and is here briefly recalled. The interconnect is a single microstrip with the signal line made by two copper traces, where a small gap between the traces is filled by graphene, in form of nanoplatelets, by using the technique shown in [16]. The microstrip layout is given in Figure 2, with its geometrical parameters reported in Table I. An FR4 dielectric has been used, with relative permittivity between 4.17 and 3.92 in the considered frequency range (up to 10 GHz). The graphene embedded in the gap is shown in Fig.3.

A procedure to retrieve equivalent electrical parameters for this graphene interconnect has been presented in [15], based on the joint use of measurements and simulations. Specifically, an equivalent relative permittivity in the range from 23 to 40 is found, by matching the computed and measured scattering parameters in the microwave range, see Fig.5. The simulations come from an equivalent model implemented with a commercial tool (CST, [17]), assuming a uniform value for the permittivity.

In the following, we use the proposed approach as an alternative way to find these equivalent permittivity values.

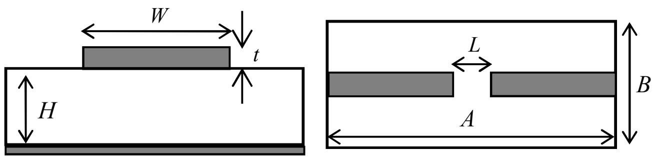

Fig. 2. The analyzed microstrip: cross section (left); upper view (right).

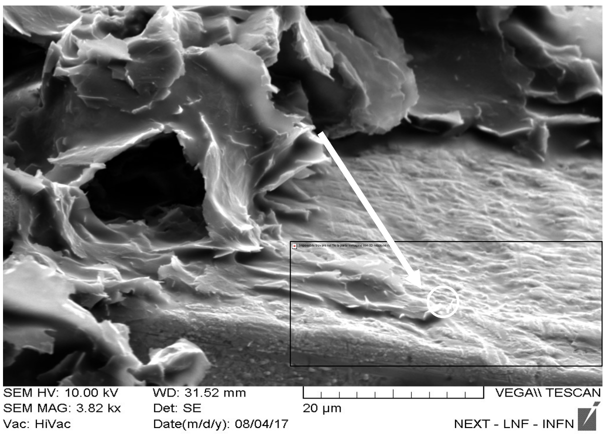

Fig. 3. Atomic microscope picture of the graphene nanoplatelets lying in the microstrip gap. Inset: the realized microstrip, with the gap highlighted.

Table 1. Values of the geometrical parameters for the microstrip.

A (*mm*)	*B* (*mm*)	*W* (*mm*)	*H* (*mm*)	*L* (*mm*)	*t* (*µm*)
50	20	1.0	0.5	0.1	14

Table 2. Velocity, characteristic impedance and p.u.l. energy for case-study 1.

microstrip	*v* (*10⁸ m/s*)	*Z₀* (Ω)	*U* (*pJ/m*)
Original	1.78	94.48	29.65
Equivalent	1.78	94.35	29.56

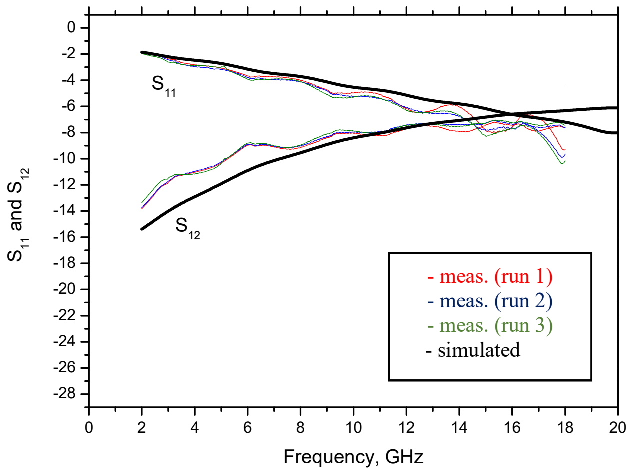

Fig. 4. Comparison between simulated vs measured scattering parameters, for retrieving the equivalent electrical permittivity [15].

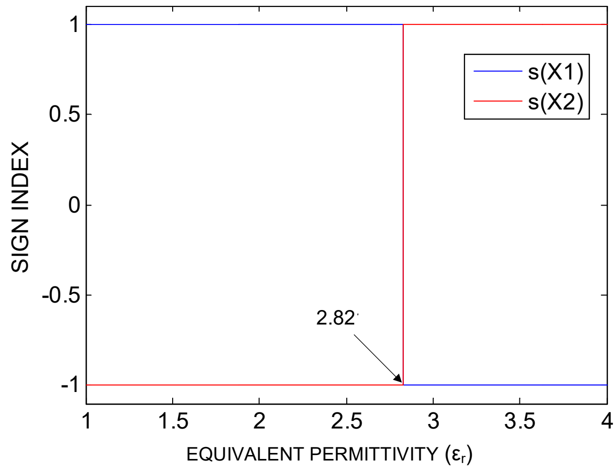

Fig. 5. Behavior of the sign indexes associated to the matrices $\mathbf{X_1}$ and $\mathbf{X_2}$ versus the equivalent relative permittivity, for the case-study 1 (microstrip without gap and without graphene). The transition region reduces to a single point, corresponding to the desired value of the equivalent permittivity.

B. Homogenization of the graphene microstrip

In order to introduce the procedure, let us first refer to the microstrip in Fig.2 without graphene (case-study 1), assuming a copper trace without gap, and considering the geometrical parameters in Table 1. The relative permittivity ranges from 1 (the external region of the microstrip) to 4.17 (the maximum value of the FR4 dielectric). These extremal values are taken as starting points for the identification procedure.

The TL parameters for a single microstrip are known in a closed form [4], and thus the matrices $\mathbf{X_1}$ and $\mathbf{X_2}$ in (6)-(7) may be easily computed. The homogenization procedure targets contemporarily the above two matrices, by deriving the corresponding sign indexes, defined as in (10). Figure 5 shows the behavior of the two sign indexes, as a function of the equivalent relative permittivity: the transition region reduces to a single value: $\bar{\varepsilon}_{r1} = \bar{\varepsilon}_{r2} = 2.82$, which is in agreement with the value, $\bar{\varepsilon}_r = 2.80$, provided by classical semi-analytical approximations available for a single microstrip, e.g. [18].

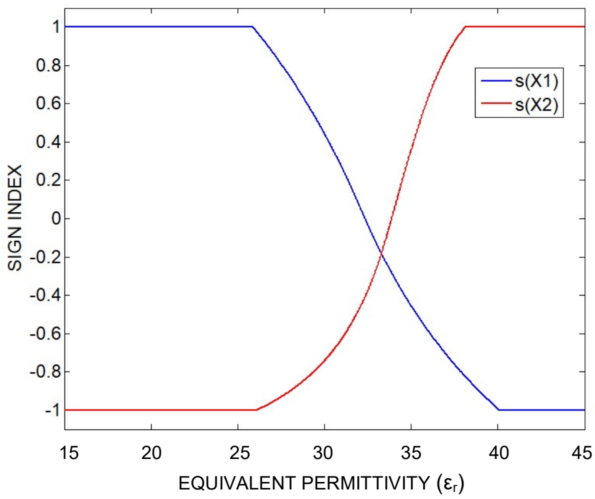

Fig. 5. Behavior of the sign indexes associated to the matrices $\mathbf{X}_1$ and $\mathbf{X}_2$ versus the equivalent relative permittivity, for case-study 2 (graphene microstrip). The transition region is here an interval.

Table 3. Equivalent permittivity values for case-study 2, with Ref. [15]

	$\bar{\varepsilon}_1$	$\bar{\varepsilon}_2$
This paper	26.5	39.5
Ref. [15]	23	40

Table 2 summarizes the results of the comparison between the propagation properties of the two lines (the per-unit-length energy refers to the application of a voltage of 1V at one line end, with the other one short-circuited).

Let us now apply the procedure to the graphene microstrip (case-study 2): in this case, the relative permittivity range is much wider, since the graphene composites may exhibit ε_r of the order of hundreds [15]. For the graphene microstrip the procedure starts from the knowledge of the measured scattering parameters, see Fig.4. The scattering matrix **S** is equivalent to any other matrix representation of the TL: for instance, **S** is related to the impedance matrix **Z** as follows [4]-[5]:

$$\mathbf{S} = [\mathbf{Z} + \mathbf{Z}_0]^{-1}[\mathbf{Z} - \mathbf{Z}_0]. \quad (13)$$

As a consequence, the measured results provide the reference matrices $\widetilde{\mathbf{X}}$ to be used in (10). In this case, there is no analytical solution to be used for computing the homogeneous cases. To this purpose, in the following we use the numerical results provided by the same simulation tool used for Fig.5.

Figure 6 shows the behavior of the two sign indexes, as functions of the equivalent permittivity: in this case, the transition region is the union of two intervals. Indeed, by applying (11) and (12) we obtain the equivalent values of permittivity reported in Table 3, compared to those retrieved in [15] with a different technique.

IV. Conclusions

In this paper, a novel technique has been proposed to derive equivalent homogeneous transmission line macromodel, starting from interconnects characterized by non-uniform spatial distribution of the permittivity. The technique is based on the study of the sign of an index associated to the terminal matrices. The technique has been successfully applied to a microstrip embedding a graphene contact, by using the scattering matrix to compute the sign index. The equivalent permittivity values derived here (26.5-39.5) are comparable to those obtained in literature by using a different identification technique (23-40).

Ackowledgments

This research was partially funded by EU H2020, under the Project TERASSE, H2020-MSCA-RISE, 823878

References

[1] R.E. Collin, Field Theory of Guided Waves, N. York: McGraw-Hill 1960.

[2] Y. L. Chow, J. J. Yang, D. G. Fang, G. E. Howard, "A closed-form spatial Green's function for the thick microstrip substrate," IEEE Trans. on Microwave Theory and Techniques, Vol.39, pp.588-592, Mar 1991.

[3] A.Maffucci, G. Miano, F. Villone, "Full-wave transmission line theory," IEEE Trans. on Magnetics, Vol.39, pp.1594-1597, 2003.

[4] C.R. Paul, Analysis of Multiconductor Transmission Lines, Wiley, 1994.

[5] G. Miano, A. Maffucci, Transmission Lines and Lumped Circuits, San Diego: Academic Press, 2001.

[6] B. Gustavsen and A. Semlyen, "Rational approximation of frequency domain responses by vector fitting," IEEE Trans. Power Del., vol. 14, pp. 1052–1061, Jul. 1999.

[7] P. Triverio, S. Grivet-Talocia, and A. Chinea, "Identification of Highly Efficient Delay-Rational Macromodels of Long Interconnects From Tabulated Frequency Data," IEEE Trans. Microwave Theory and Techniques, vol. 58, pp. 566–577, Mar. 2010.

[8] E. Bogatin, Signal Integrity, New Jersey: Prentice Hall, 2004.

[9] D. Vande Ginste, D. De Zutter, D. Deschrijver, T. Dhaene, P. Manfredi, F. Canavero, "Stochastic Modeling-Based Variability Analysis of On-Chip Interconnects," IEEE Trans. on Components, Packaging and Manufacturing Tech., Vol.2, pp.1182-1192, Jul. 2012.

[10] A. Todri-Sanial, J. Dijon, A. Maffucci, Carbon Nanotubes for Interconnects. The Netherlands: Springer, 2016.

[11] G. Y. Slepyan, A. Boag, V. Mordachev, E. Sinkevich, S. Maksimenko, P. Kuzhir, G. Miano, M.E. Portnoi, A. Maffucci, "Nanoscale Electromagnetic Compatibility: Quantum Coupling and Matching in Nanocircuits," IEEE Trans. on Electromagnetic Compatibility, vol.57, no.6, pp.1645-1654, Dec. 2015.

[12] J. S. Ochoa and A. C. Cangellaris, "Homogenization Technique for Transmission Lines with Random Permittivity Profiles," Proc. of 17th IEEE Work. on Signal and Power Integrity, Paris, France, May 2013.

[13] A. Maffucci, A. Vento, S. Ventre, A. Tamburrino, "A Novel Technique for Evaluating the Effective Permittivity of Inhomogeneous Interconnects Based on the Monotonicity Property", IEEE Trans. on Components, Packaging and Manufacturing, Vol.6, pp.1417-1427, Set. 2016

[14] Z. Zhou and K. L. Melde, "A Comprehensive Technique to Determine the Broadband Physically Consistent Material Characteristics of Microstrip Lines," IEEE Trans. on Microwave Theory and Techniques, Vol.58, pp.185-194, Jan 2010.

[15] S. Bellucci, A. Maffucci, S. Maksimenko, F. Micciulla, M. D. Migliore, A. Paddubskaya, D. Pinchera and F. Schettino, "Electrical Permittivity and Conductivity of a Graphene Nanoplatelet Contact in the Microwave Range," Materials, vol.11, p.2519-1-11, Dec. 2018.

[16] A. Maffucci, F. Micciulla, A. Cataldo, G. Miano, S. Bellucci, "Bottom-up Realization and Electrical Characterization of a Graphene-Based Device," Nanotechnology, Vol.27, p.095204-1-9, 2016.

[17] CST Microwave Studio, https://www.cst.com

[18] E. Hammerstad and Ø. Jensen, "Accurate Models for Microstrip Computer-Aided Design," *Proc. of Symposium on Microwave Theory and Techniques*, pp. 407-409, Jun. 1980.